Petrophysics of carbonatic and evaporitic rocks from Araripe Basin

Gurjão, K.G.R.[1]; Soares, J.A.[1]; Barbosa, J.A.[2]; Gomes, I.F. [2]; Figueiredo, A.N.[1]
[1] Universidade Federal de Campina Grande, [2] Universidade Federal de Pernambuco

This paper was prepared for presentation during the 13th International Congress of the Brazilian Geophysical Society held in Rio de Janeiro, Brazil, August 26-29, 2013.

Abstract

This paper presents petrophysical properties measured on rock samples from Araripe basin, located on northwestern inlands of Brazil. Rock types are basically limestones, dolomites and gypsum. Analyzed properties are porosity, grain density, total density, elastic wave velocities and elastic moduli. Rock samples were prepared and tested in laboratory under dried condition, room temperature and effective confining pressures up to 40 MPa. The majority of these rocks are tight ones with porosity limited to 14%, several of them with porosity lower than 3%. Grain density showed to be a very useful parameter for rock typing. Total density is sensitive to porosity and grain density while elastic wave velocities and moduli are sensitive not only to porosity but also to other variables.

Introduction

This paper shows the results obtained in a field campaign and laboratory tests to characterize the physical properties of carbonatic and evaporitic rocks which occur at Araripe Basin, located at northeastern of Brazil. This activity is part of a R&D project being conducted by the Federal University of Campina Grande (UFCG) and promoted by PETROBRAS. Petrophysical analyses presented here were performed at the UFCG´s Laboratory of Petrophysics on samples collected from outcrops by researchers of the Federal University of Pernambuco (UFPE). Two sets of rock samples were sent to UFCG, the first one was composed of hand samples, and the second one was composed of field cut plugs. Prior to laboratory physical analyses, the former rock set was submitted to plug preparation, while the later was submitted only to rectification of the plug extremities in order to guarantee perfectly plane and parallel plug faces. The properties investigated until the moment of this paper are porosity, grain density, total density, elastic wave velocities and elastic moduli of 64 plugs.

The paleozoic Araripe basin contains carbonatic and evaporitic rocks into its aptian-albian stratigrafic sequence (ASSINE, 1992). Outcrops of this sequence were sampled for petrophysical analyses. The study area, which have good outcrops of the stratigraphic units chosen corresponds to the portion north and south of the western domain of the Araripe basin, located at the states of Pernambuco and Ceará (Figure 1). Chosen units represent two stages of the lacustrine system developed between the aptian and albian: Crato and Ipubi formations. The Ipubi formation is mainly composed of gypsum and anhydrite and their deposits are intensely affected by faulting and fracturing processes. In general faults and fractures are filled by fibrous gypsum and clay. The Crato Formation, which is also affected by faults and fractures, is composed of six cycles of laminated carbonates interleaved with levels of shales and marls (NEUMANN, 1999). This study will focus on laminated carbonates and gypsum levels that occur in the upper portion of these units.

Method

Cylindrical plugs with one-half inch in diameter and about 5 cm in length were prepared using saw, a portable diamond bit engine drill and a plug face rectifier (Figure 2). After their preparation, plugs were subjected to oven drying for 24 hours under 80℃ of temperature, geol ogical description, weighted on a semi-analytic electronic scale and their dimensions (diameter and length) were measured with a digital caliper.

Afterwards to these initial procedures, laboratory assays were performed in a gas poropermeameter (Figure 3a). Using a matrix cup (Figure 3b) plug grain volumes and porosities were measured. The difference between the plug total volume, calculated from its dimensions, and its grain volume is the pore volume of the sample. The plug porosity is directly obtained by the ratio between the pore volume and the total plug volume.

Once the sample is dried, one may assumes that its mass corresponds to the mass of its solid phase, being the grain density given by the ratio between the plug mass and its measured grain volume. Known porosity and grain density, bulk density can be estimated ignoring the density of the air which fills the rock pores.

The grain volume is measured by the expansion of a volume of nitrogen housed in one chamber inside the gas poropermeameter, obeying the Boyle law, with a constant temperature.

The elastic properties essays were realized by measuring the transit time of the direct transmission of P and S waves through the axial length of the analyzed plugs. The equipment (Figure 4) allows rock tests under controlled confining and pore pressures, temperature and fluid saturation. In this study the measurements of P and S wave velocities were carried out on dried plugs subjected to decreasing levels of confining effective pressure, from 40 MPa to 5 MPa. Pore pressure and temperature were maintained at room levels. Determined the transit times of the waves and known the length of the plugs, wave velocities are given by the ratio of these parameters.

Elastic velocities were measured under effective pressure range from 5 to 40 MPa and porosity was measured at room pressure. To examine velocity variation with porosity under high levels of pressure, an estimation of porosity was done to pressures until 40 MPa. This was done considering the incompressibility for each level of effective pressure, which is calculated from the measured wave velocities and bulk density, as presented by BOURBIÉ *ET AL.* (1987). In addition to compressibility, the Young modulus, the shear modulus and the Poisson´s ratio were also calculated.

Results

Figure 6 shows grain density values measured for all analyzed plugs. From this figure can be observed that grain density of limestone plugs was approximately 2.7g/cc, while grain density of gypsum ones was around 2.3g/cc. But three gypsum plugs, which were extracted from the same outcrop, present grain density between the gypsum and the limestone grain densities. This was interpreted as an indication of a mineralogical matrix composed by a mixture of limestone and gypsum. This assumption should be proved through chemical analysis. Calcite, which is the mineralogical matrix of limestone, presented average grain density similar to limestone, while dolomite, that is also a carbonatic rock with higher grain density in comparison with limestone, presented the same property around 2.8 g/cc.

Figure 7 shows the relationship between total density and porosity under room temperature and pressure. Analyzing this figure we verify that, in general, as the porosity increases the total density decreases. In this figure a very representative linear fit is showed for the case of limestone ($R^2 = 0.99$). As the number of dolomite plugs is very small, a reliable fit was not found for this these plugs, although these plugs show higher total density for a given porosity value in comparison with the limestone ones. This is the grain density effect since there is no fluid variation. Though there are 23 plugs of gypsum, all of them have very small porosity, limited to 3%, so it was not defined a good fit for this rock type. This figure suggests that some gypsum plugs are composed indeed by a mixture of gypsum and some kind of carbonate.

Figure 8 presents the relationship between P wave velocity (VP) and porosity for 40 MPa of confining pressure. In general VP tends to decrease while porosity increases, but with a high dispersion. This occurs because wave velocities are dependent on some other variables beyond porosity. Can be noted that for a similar range of porosity dolomite plugs show higher P wave velocities than the limestone ones and that the calcite plugs are faster than the gypsum ones.

The system used for wave velocity measurements is able to propagate into the rock plugs two S waves, each of them with direction of polarization perpendicular to another. Figures 9 and 10 present relationships between porosity and S_1 and S_2, respectively. The same observations made for Figure 8 can also be applied for these figures.

Figure 11 shows the ratio of VS_1/VS_2 against porosity. This is used for analysis of the possible occurrence of elastic anisotropy. The rock is considered isotropic when this ratio is near 1, while it is more anisotropic when this ratio increases or decreases far way from 1. This figure shows that the limestone plugs are near isotropic, while those of gypsum may be fairly anisotropic. This feature probably is due to the occurrence of fibrous gypsum filling fractures or may be caused by the fractures themselves.

Figures 12, 13, 14 and 15 present the elastic moduli against porosity, namely Young´s modulus, shear modulus, incompressibility and Poisson´s ratio, respectively. Analyzing these graphics one can infers that the general behavior of these moduli is their decreasing with the porosity increasing, although their high degrees of dispersion suggest these moduli are affected by other variables besides porosity. It should be emphasized that these results are valid only for dried samples.

Conclusions

For the rock samples presented in this paper porosity values measured under room temperature and pressure are in the range of 0.45% to 22.8%, whose samples with higher values are limestones and dolomites, and those with lower values are gypsum and calcites. Grain density is a very useful parameter for rock typing. Plugs analyzed here presented grain density around 2.7 g/cc for limestone e calcite ones, 2.8 g/cc for dolomite and 2.3 g/cc for gypsum. Total density is very sensitive to porosity and grain density. A reliable linear fit relating porosity and total density was established for the analyzed limestone plugs. In general wave velocities decrease with porosity increasing, but the high dispersion of this relationship indicates that wave velocities are dependent on some other variables beyond porosity. For a same porosity value, dolomite tends to be faster than limestone which is faster than gypsum. This occurs mainly due to the grain density effect. This study showed that the limestone plugs from Araripe basin are near isotropic, while those of gypsum may be fairly anisotropic. This is probably due to the occurrence of fibrous gypsum filling fractures. Elastic moduli also decrease with porosity increasing, although their high degrees of dispersion suggest these moduli are affected by other variables besides porosity.

Acknowledgments

Authors thank project number 0050.0078516.12.9 and PETROBRAS for financial support and permission for this publication. The first author thanks CNPq for financial aid.

References

ASSINE, M.L. (1992). Análise Estratigráfica da Bacia do Araripe, Nordeste do Brasil. Revista Brasileira de Geociências,Curitiba- PR, v. 22, p. 289-300.

BOURBIÉ, T.; COUSSY, O.; ZINSZNER, B. (1987). Acoustics of porous media.ÉditionsTechnip.France.

NEUMANN, V.H. (1999). Estratigrafía, sedimentología, geoquímica y diagénesis de los sistemas lacustres Aptiense-Albienses de la cuenca de Araripe (Noreste de Brasil). Barcelona, 247 p. Tese (Doutorado) – Facultat de Geologia – Universitat de Barcelona.

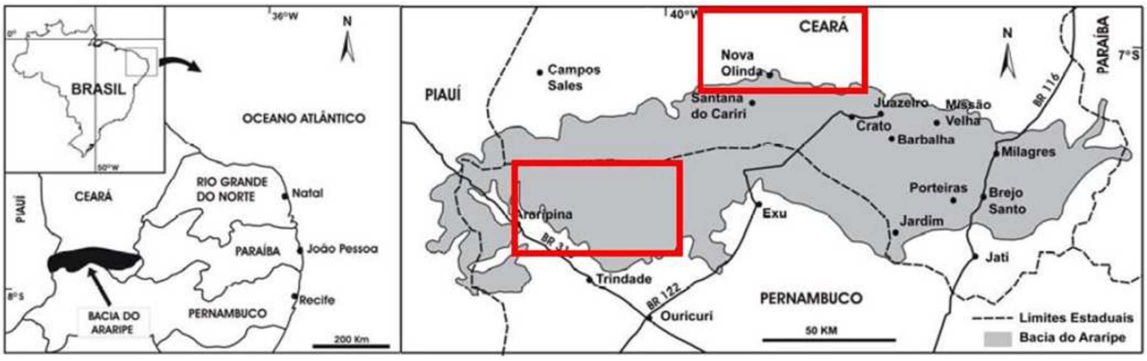

Figure 1 – Localization map of the Araripe Basin. Visited outcrops locations are marked in red.

Figure 2 - Equipments used for plug preparation: a) saw; b) portable diamond bit engine drill; c) plug rectifier.

Figure 3 - Equipments used for grain density and porosity measurements: a) gas poropermeameter; b) matrix cup; c) semi-analytic precision scale.

Figure 4 - System used for measuring of rock elastic properties.

Figure 5 - Example of carbonatic and evaporitic plugs analyzed in this paper.

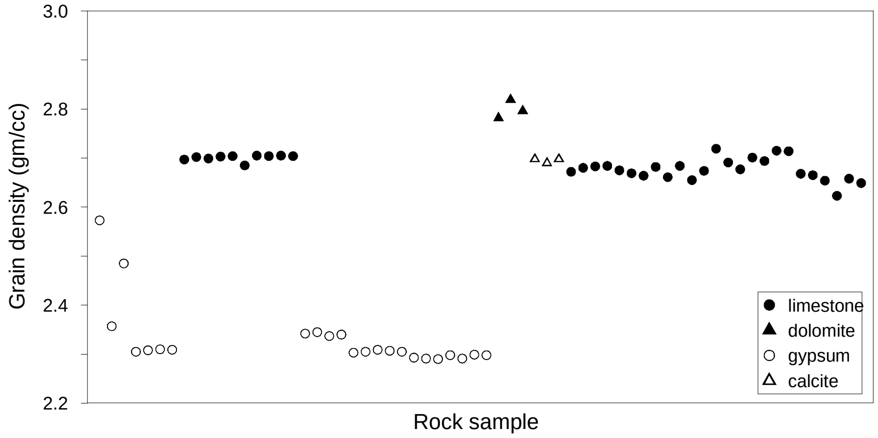

Figure 6 - Grain density of carbonatic and evaporitic rocks from Araripe Basin.

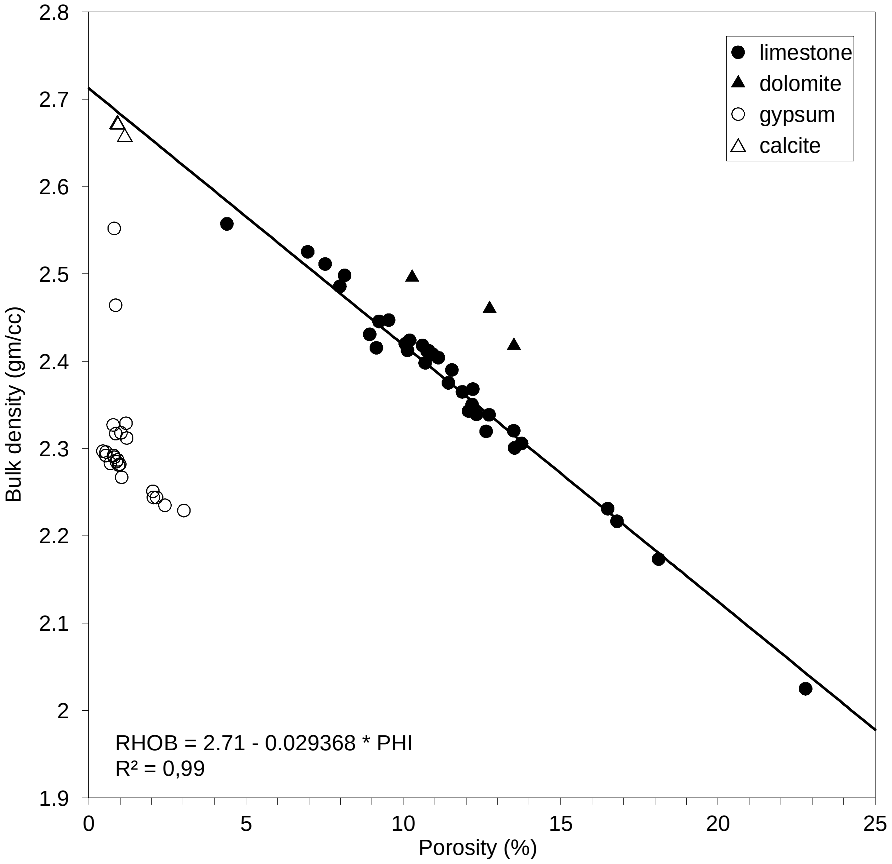

Figure 7 - Relationship between bulk density and porosity, both measured under room pressure.

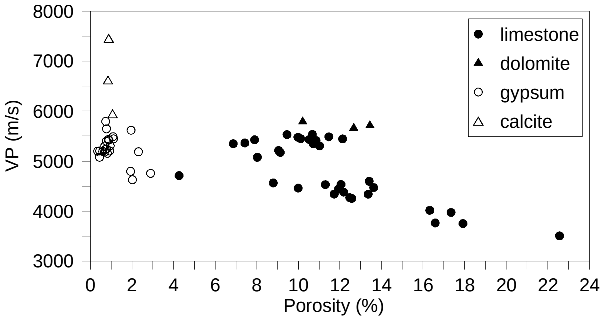

Figure 8 - P wave velocity versus porosity for effective confining pressure of 40 MPa.

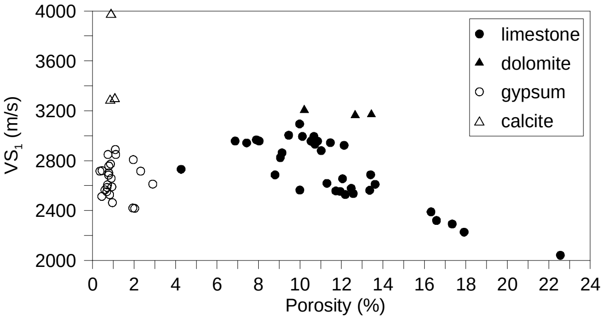

Figure 9 – S_1 wave velocity versus porosity for effective confining pressure of 40 MPa.

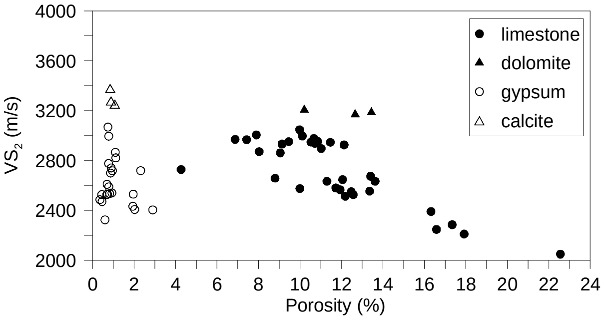

Figure 10 – S_2 wave velocity versus porosity for effective confining pressure of 40 MPa.

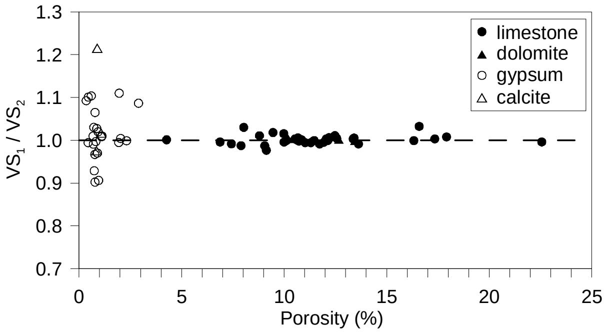

Figure 11 – Ratio VS_1/VS_2 versus porosity for effective confining pressure of 40 MPa.

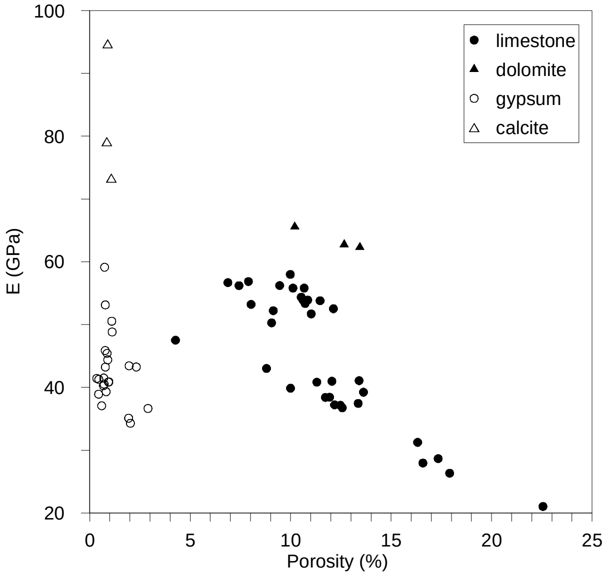

Figure 12 – Young´s modulus and porosity for effective confining pressure of 40 MPa.

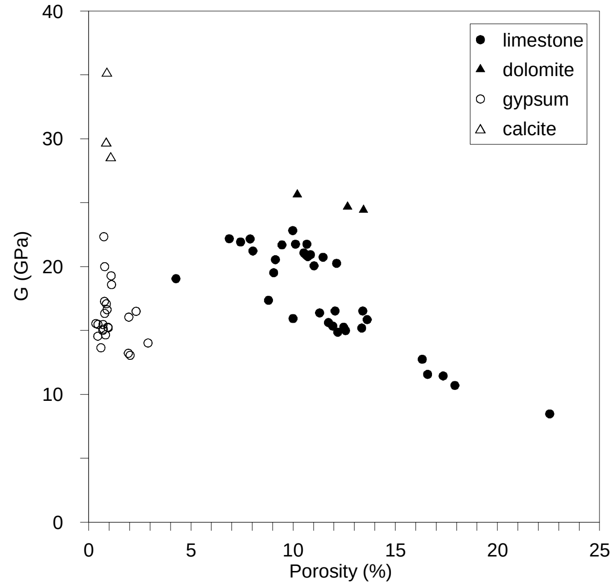

Figure 13 – Shear modulus and porosity for effective confining pressure of 40 MPa.

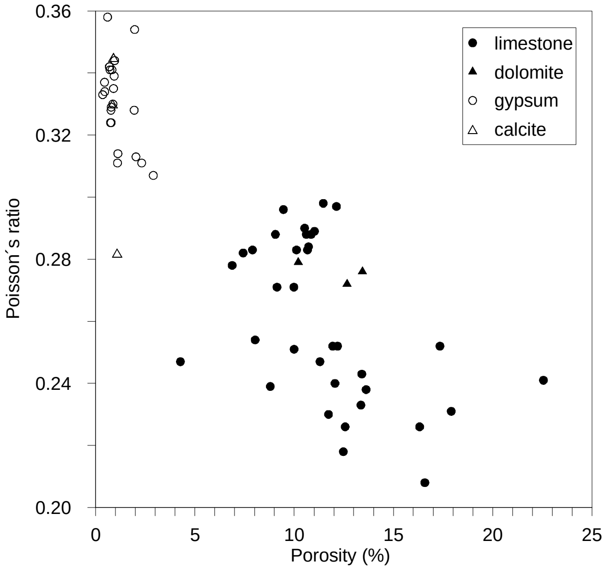

Figure 15 – Poisson´s ratio and porosity for effective confining pressure of 40 MPa.

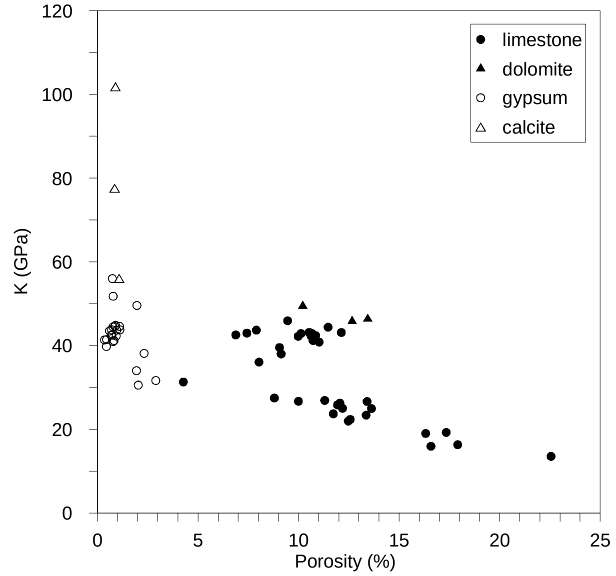

Figure 14 – Incompressibility and porosity for effective confining pressure of 40 MPa.